Binary Carbonyls of Platinum, $Pt(CO)_n$ (Where n = 1–4). A Comparative Study of the Chemical and Physical Properties of $M(CO)_n$ (Where M = Ni, Pd, or Pt; n = 1–4)

Ernst P. Kündig, Douglas McIntosh, Martin Moskovits,* and Geoffrey A. Ozin*

Contribution from the Lash Miller Chemical Laboratories and Erindale College, University of Toronto, Toronto, Ontario. *Received May 4, 1973*

Abstract: The products of the cocondensation reactions of Pt atoms with CO at 4.2–10°K are investigated by matrix infrared spectroscopy and are shown to be binary carbonyl complexes of the form $Pt(CO)_n$. Examination of the reaction products in pure $^{12}C^{16}O$, in $^{12}C^{16}O/^{13}C^{16}O$, and in dilute $^{12}C^{16}O$/Ar and $^{12}C^{16}O/^{13}C^{16}O$/Ar matrices establishes the stoichiometry of the products to be respectively n = 1–4. Isotopic frequencies and integrated infrared intensities are computed for the CO stretching modes of $Pt(^{12}C^{16}O)_n(^{13}C^{16}O)_{4-n}$ (n = 0–4) on the basis of the Cotton–Kraihanzel force field approximation and on isotope intensity sum rules and are found to be in close agreement for a molecule with regular tetrahedral (T_d) symmetry. Similar frequency calculations are performed on the Pt(CO) ($C_{\infty v}$), $Pt(CO)_2$ ($D_{\infty h}$), and $Pt(CO)_3$ (D_{3h}) complexes. Because of spectral overlaps the last compound is not well characterized. The data for the series of complexes $Pt(CO)_n$ (n = 1–4) and the corresponding data for $Ni(CO)_n$ and $Pd(CO)_n$ are compared in terms of the trends in their force constants, structure, stabilities, and bonding properties. The relationship of the MCO data to CO chemisorbed on M (M = Ni, Pd, and Pt) is also discussed.

Nickel tetracarbonyl was the first metal carbonyl to be prepared.[1] Moreover it holds great industrial and chemical importance by way of the Mond process and the many organic catalytic carbonylation and decarbonylation reactions. Despite this fact it was not until 1972 that the first definitive evidence[2,3] for the existence of its congeners $Pd(CO)_4$ and $Pt(CO)_4$ was reported. Two independent groups,[4,5] using matrix isolation infrared and Raman techniques, reported data for the products of the Pd atom CO and CO/Ar matrix cocondensation reactions and were able to characterize the series of binary complexes $Pd(CO)_n$ (where n = 1–4) analogous to $Ni(CO)_n$. The most stable palladium carbonyl in this series was shown from warm-up and mixed isotope experiments to be the tetracarbonyl molecule $Pd(CO)_4$, having regular tetrahedral (T_d) symmetry. $Pd(CO)_4$ was found to be thermally unstable as compared with $Ni(CO)_4$. This presumably is the reason for previous failures to prepare $Pd(CO)_4$ by conventional techniques. Recently too, matrix infrared and Raman evidence was reported[6] for the existence of platinum tetracarbonyl $Pt(CO)_4$, formed in the cocondensation reaction of Pt atoms with either *pure* CO at 4.2–10°K or dilute CO/Ar mixtures which had been deposited or annealed at 30°K. The infrared and Raman activities and matrix Raman depolarization measurements were those expected for a tetracarbonyl $Pt(CO)_4$ having regular tetrahedral symmetry.

In this paper we have extended our infrared experiments of the palladium–carbon monoxide system to the Pt/CO and Pt/CO/Ar matrix cocondensation reactions. Using variable concentration, warm-up, and $^{13}C^{16}O$ isotope substitution experiments, we have been able to prepare and characterize $Pt(CO)_4$ as well as the intermediate binary carbonyls $Pt(CO)_n$ (where n = 1–3). Moreover, the platinum series serves to complete the spectroscopic data for the group of complexes $M(CO)_n$ (where M = Ni, Pd, or Pt; n = 1–4), which enables us to examine the trends in their vibrational spectra, force constants, structures, stabilities, and bonding properties.

(1) L. Mond, C. Langer, and F. Quincke, *Trans. Chem. Soc.*, **57**, 749 (1890).
(2) H. Huber, P. Kündig, M. Moskovits, and G. A. Ozin, *Nature (London), Phys. Sci.*, **235**, 98 (1972).
(3) J. H. Darling and J. S. Ogden, *Inorg. Chem.*, **11**, 666 (1972).
(4) P. Kündig, M. Moskovits, and G. A. Ozin, *Can. J. Chem.*, **50**, 3587 (1972).
(5) J. S. Ogden, private communication.
(6) P. Kündig, M. Moskovits, and G. A. Ozin, *J. Mol. Struct.*, **14**, 137 (1972).

Experimental Section

Monatomic platinum vapor was obtained by directly heating with ac a 0.030-in. tungsten rod around the center of which were wound several turns of 0.010-in. Pt wire. The platinum metal (99.99%) was supplied by McKay Inc., New York. Research grade $^{12}C^{16}O$ (99.99%) and Ar (99.99%) were supplied by Matheson. Isotopically enriched $^{13}C^{16}O$ (55%) was supplied by Miles Research Laboratories.

The rate of metal atom depositions was continuously monitored and controlled using a quartz crystal microbalance. The deposition rate was set such that the probability of a metal atom having another metal atom as nearest neighbor in the argon lattice was approximately 1:1000. Matrix gas flows, controlled by a calibrated micrometer needle valve, were maintained in the range 2–8 mmol/hr. In the infrared experiments the matrices were deposited on a CsI window cooled to either 4.2°K by an Air Products liquid helium cryotip transfer system or to 10°K by means of an Air Products Displex closed cycle helium refrigerator. Ir spectra were recorded using Perkin-Elmer 180 and Beckman IR-12 spectrophotometers.

Results

Platinum Tetracarbonyl, $Pt(CO)_4$. When Pt atoms were cocondensed with pure $^{12}C^{16}O$ at 10°K a strong absorption at 2047.8 cm^{-1} with a weak shoulder at 2055.0 cm^{-1} was observed in the matrix infrared spectrum. The corresponding matrix Raman experiment showed an unresolved broad line centered at about 2049 cm^{-1} and a weaker line at 2119 cm^{-1} where the former was depolarized and the latter was "totally" polarized (Figure 1). Although the matrix infrared and Raman activities and depolarization measurements for the Pt/CO cocondensation reaction are consistent with the product being a regular tetrahedral tetracar-

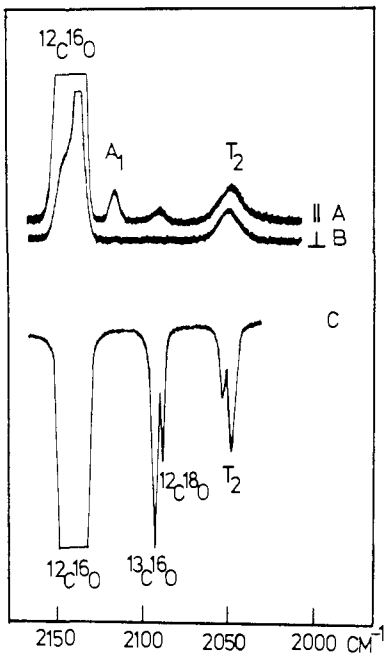

Figure 1. The matrix Raman and infrared spectra of the products of the cocondensation reaction of Pt atoms with $^{12}C^{16}O$ at 4.2°K: (A) Raman parallel, (B) Raman crossed polarization, and (C) infrared, showing $Pt(^{12}C^{16}O)_4$.

bonyl, one cannot rule out the product's being a tricarbonyl $Pt(CO)_3$ or a dicarbonyl $Pt(CO)_2$ species, both of which could have yielded spectra similar to those observed.

Before a detailed investigation of binary intermediate carbonyls or platinum becomes feasible, the stoichiometry of the reaction product in *pure* CO (which is expected to be the complex with highest coordination number) must be established from mixed $^{12}C^{16}O/^{13}C^{16}O$ isotope substitution experiments.

In an attempt to avoid lattice distortion problems arising from the low substitutional site symmetry in pure CO matrices (usually referred to as matrix splitting), the mixed isotope experiments were performed in "concentrated" carbon monoxide–argon matrices, which had been deposited with Pt atoms at 20–25°K. This technique, which essentially allows the matrix to anneal during the deposition, has proved successful in the related $Ni(N_2)_4$ system[7] and appears to be working in the Pt/CO/Ar system as seen by the appearance of a *single* absorption at 2053.3 cm^{-1} in $^{12}C^{16}O$:Ar = 1:10 rather than the matrix split at 2055.0:2047.8 cm^{-1} in pure $^{12}C^{16}O$.

When Pt atoms were cocondensed with $^{12}C^{16}O$: $^{13}C^{16}O$:Ar ≃ 1:1:20 at 20–25°K (Figure 2), the matrix infrared spectrum shows five lines (a very weak line was observed at approximately 2108 cm^{-1} (see Figure 2A and Table I)) at 2053.3, 2033.0, 2021.9, 2013.9, and 2006.9 cm^{-1} as well as the two very intense absorptions at 2138 and 2093 cm^{-1} due to unreacted $^{12}C^{16}O$ and $^{13}C^{16}O$. It has been shown that the maximum number of distinct infrared CO stretching modes expected for tetracarbonyl mixed isotopic molecules $M(^{12}C^{16}O)_n(^{13}C^{16}O)_{4-n}$ (where n = 0–4) is eight. One can then tentatively assign the *five* observed lines listed above to these species. The three missing lines are presumably not observed because of overlap with the unreacted $^{13}C^{16}O$ line.

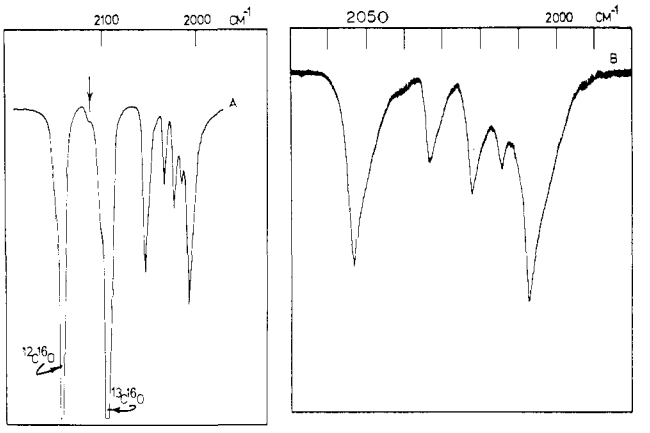

Figure 2. The matrix infrared spectrum of the products of the cocondensation reaction of Pt atoms with $^{12}C^{16}O$:$^{13}C^{16}O$:Ar = 1:1:20 at 20–25°K showing the formation of the species $Pt(^{12}C^{16}O)_n(^{13}C^{16}O)_{4-n}$ (where n = 0–4): (A) complete spectrum, normal scan, (B) high resolution scan of 2060–2000-cm^{-1} region.

Table I. Isotopic Frequency and Infrared Absorption Intensity Calculations for the CO Stretching Modes of $Pt(^{12}C^{16}O)_n(^{13}C^{16}O)_{4-n}$ (n = 0–4) in Solid Argon and Best Fit C–K Force Constants[a]

Obsd freq	Calcd freq	Obsd[b] intensity	Calcd intensity	Assignment
2006.9	2007.2	10.000	10.000	III(B_2) + IV(E) + V(T_2)
2013.9	2014.0	1.615	1.303	II(A_1)
2021.9	2022.2	3.281	2.461	III(A_1)
2033.0	2032.7	1.856	2.420	IV(A_1)
2053.3	2052.8	6.258	6.561	I(T_2) + II(E) + III(B_1)
	2088.1		0.015	IV(A_1)
	2099.0		0.317	III(A_1)
~2108[c]	2107.4		0.074	II(A_1)

Notation	Isotopic molecule	Point symmetry
I	$Pt(^{12}C^{16}O)_4$	T_d
II	$Pt(^{12}C^{16}O)_3(^{13}C^{16}O)$	C_{3v}
III	$Pt(^{12}C^{16}O)_2(^{13}C^{16}O)_2$	C_{2v}
IV	$Pt(^{12}C^{16}O)(^{13}C^{16}O)_3$	C_{3v}
V	$Pt(^{13}C^{16}O)_4$	T_d

[a] The best fit C–K CO force constants were k_{CO} = 17.28 and $k_{CO,CO}$ = 0.26 mdyn/Å. [b] The observed intensities were measured by assuming a triangular contour for the infrared band and using the expression $I = \Delta\nu_{1/2}[1 + \gamma \log \gamma/(1 - \gamma)]$, where $\Delta\nu_{1/2}$ = width of the infrared band at half-height, γ = fractional transmittance, and $I = \int \ln \gamma d\nu$. [c] Very weak line indicated by an arrow in Figure 2A.

Frequency and Intensity Calculations for Isotopically Substituted $Pt(^{12}C^{16}O)_n(^{13}C^{16}O)_{4-n}$ (n = 0–4). The eight-line spectrum (in the CO stretching region) expected for a tetrahedral tetracarbonyl molecule, formed in a mixed ^{12}CO:^{13}CO = 1:1 isotope experiment, is due to the five possible isotopically related molecules listed in Table I.

A least-squares analysis was performed on the observed five-line spectrum discussed above assuming the Cotton–Kraihanzel approximation[8] and adjusting the values of the two parameters k_{CO} and $k_{CO,CO}$. The observed and calculated frequencies are compared in

(7) H. Huber, E. P. Kündig, M. Moskovits, and G. A. Ozin, *J. Amer. Chem. Soc.*, **95**, 332 (1973).

(8) F. A. Cotton and C. S. Kraihanzel, *J. Amer. Chem. Soc.*, **84**, 4432 (1962).

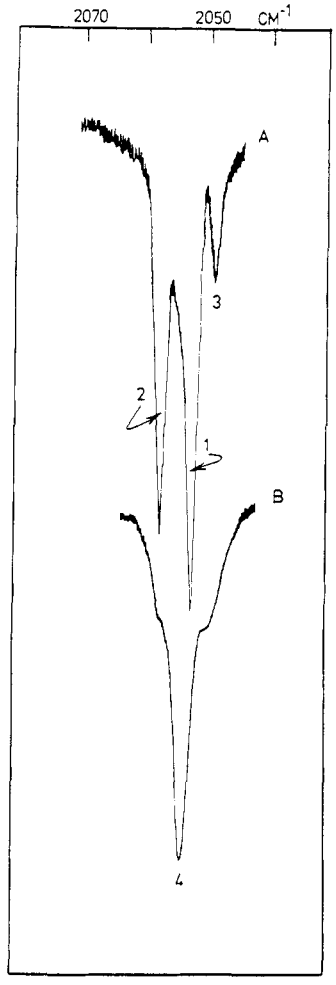

Figure 3. The matrix infrared spectrum of the products of the concondensation reaction of Pt atoms with $^{12}C^{16}O$:Ar = 1:250: (A) at 10°K, and (B) after warm-up to 35°K.

Table I. The calculation predicts that at least two of the three "missing" lines are obscured by the strong $^{13}C^{16}O$ absorption. The intensities of these absorptions can also be predicted from the well-known intensity sum rules[9] used by Haas and Sheline[10] and more recently by Ogden[11] and Ozin and Moskovits, *et al.*[7] The relative intensities predicted on the basis of tetrahedral geometry are listed in Table I as are the observed absorbances. The absorption predicted at 2107.4 cm^{-1} is not obscured by the ^{13}CO band. It is calculated to be very weak and is indeed observed as a very weak line at approximately 2108 cm^{-1}.

The calculation indicates that there is good agreement between calculated and observed frequencies and intensities when tetrahedral geometry is assumed providing simultaneous support both for the vibrational assignments as well as the assumed structure. We therefore conclude that $Pt(CO)_4$ is a regular tetrahedral molecule.

Intermediate Binary Carbonyls of Platinum, $Pt(CO)_n$ (Where n = 1–3). Having established the identity of $Pt(CO)_4$, it would appear at first sight to be a relatively simple matter to synthesize and define the lower coordination complexes $Pt(CO)_n$ (n = 1–3) by variable concentration, warm-up, and isotopic substitution experiments, similar to those applied to the analogous $Ni(CO)_n$[12] and $Pd(CO)_n$[4] complexes.

However, the Pt/CO/Ar system provided a number of problems which were not encountered in the analogous Ni and Pd experiments. In order to obtain a satisfactory set of Pt/CO/Ar data, a number of control runs were necessary. Complications arose because of the following two factors: (i) for all $Pt(CO)_n$ (n = 1–4) molecules, the CO stretching modes are observed within a very narrow frequency range (2057–2049 cm^{-1}) and accidental overlap of lines, especially in mixed isotope experiments, was inevitable; (ii) in the process by which Pt was vaporized it was impossible to avoid "trace" carbon dioxide contamination of the matrices. Although Pt atoms and CO_2 were shown *not* to complex under conditions of matrix isolation, it was found that $Pt(CO)_n$ and CO_2 can form "weak" complexes of the type $Pt(CO)_n(CO_2)_m$, which contributed spurious lines and which had to be identified and accounted for in the analysis of $Pt(CO)_n$.

The following experiments were undertaken which led to the synthesis, assignment of lines, and characterization of the lower binary carbonyls of platinum.

When Pt atoms were cocondensed with dilute $^{12}C^{16}O$:Ar ≃ 1:250 mixtures, the matrix infrared spectrum (Figure 3) showed a prominent absorption at 2052 cm^{-1} with a weaker absorption at 2058 cm^{-1}. Weak lines at about 2039[12a] and 2001.8 cm^{-1} also appeared in the spectra with intensities which seemed to be CO_2 dependent. The possibility of these weak lines arising from a hydride impurity (ν_{PtH} stretching modes are expected in the 2000-cm^{-1} region) was checked by cocondensing Pt atoms with H_2:Ar ≃ 1:250 mixtures. Absorptions in the 2000-cm^{-1} region were *not* observed and the possibility of these lines being Pt–H stretching modes was eliminated.

Experiments were conducted in which Pt atoms were cocondensed with pure CO_2 and various CO_2/Ar mixtures. Absorptions which could be assigned to binary $Pt(CO_2)_n$ complexes could not be detected (a result which parallels an earlier negative report for the Ni/CO_2 system[13]). However, when Pt atoms were cocondensed with CO:CO_2:Ar ≃ 1:1:500 mixtures, the feature at 2039 cm^{-1} became a major line in the spectrum, indicating that it was probably associated with mixed complexes of the type $Pt(CO)_n(CO_2)_m$. Warm-up experiments suggested that the CO_2 was bound less strongly than the CO as the absorption(s) associated with these "mixed" complexes rapidly decreased in intensity relative to the $Pt(CO)_n$ absorptions and had disappeared when $Pt(CO)_4$ predominated. These data indicate that during warm-up, CO_2 is either eliminated from the complex or displaced by CO diffusing in the matrix. Thus the lines at 2039 and probably 2001.8 cm^{-1} are not associated with the $Pt(CO)_n$ species.

When the matrix shown in Figure 3 is allowed to warm up in the range 10–20°K a new line at 2049 cm^{-1}

(9) E. B. Wilson, J. C. Decius, and P. C. Cross, "Molecular Vibrations," McGraw-Hill, New York, N. Y., 1955; B. Crawford, Jr., *J. Chem. Phys.*, **20**, 977 (1952).
(10) H. Haas and R. K. Sheline, *J. Chem. Phys.*, **47**, 2996 (1967).
(11) J. H. Darling and J. S. Ogden, *J. Chem. Soc., Dalton Trans.*, 2496 (1972).
(12) R. L. DeKock, *Inorg. Chem.*, **10**, 1205 (1971).
(12a) NOTE ADDED IN PROOF. Recent studies by us have shown that the line at 2039 cm^{-1} is either partly or completely due to traces of $^{13}C^{18}O$ present in commercially available $^{12}C^{16}O/^{13}C^{16}O$ mixtures.
(13) H. Huber, M. Moskovits, and G. A. Ozin, *Nature (London), Phys. Sci.*, **236**, 127 (1972); **239**, 48 (1972).

begins to grow in. Furthermore, the line at 2052 cm^{-1} *grows* in intensity and begins to *shift* to 2053 cm^{-1}. The line at 2058 cm^{-1} is usually the first to disappear on warm-up to 25–30°K and is followed by the line at 2049 cm^{-1}, leaving a very strong absorption at 2053 cm^{-1}, which is clearly associated with the most stable complex and is coincident with the T_2 mode of $Pt(CO)_4$.

Although the CO stretching modes observed in dilute CO/Ar experiments lie within a frequency range of about 10 cm^{-1}, *four* modes could be identified at 2058, 2053, 2052, and 2049 cm^{-1} and are associated with binary platinum carbonyl complexes.

A reasonable conclusion is therefore that all *four* species of $Pt(CO)_n$ are formed in the Pt/CO/Ar matrix reaction, the most stable being $Pt(CO)_4$ (2053 cm^{-1}). With these data alone a tentative assignment of the four observed bands to the $Pt(CO)_n$ species can be made on the basis of their relative intensities on deposition and their warm-up characteristics. Assuming intuitively that at dilution of CO:Ar $\simeq$ 1:250 the relative probability of forming $Pt(CO)_n$ decreases monotonically with increasing n (by analogy with $Pd(CO)_n$, see ref 4), then the *strongest* line observed on deposition at 2052 cm^{-1} can be ascribed to $Pt^{12}C^{16}O$ with the weaker line at 2058 cm^{-1} assigned to $Pt(^{13}C^{16}O)_2$. The new line at 2049 cm^{-1} that grows in on warm-up is therefore assigned to $Pt(^{12}C^{16}O)_3$. It is noteworthy that the concentration of the tricarbonyl species (as measured by the absorbance of the line at 2049 cm^{-1}) is never very large implying a low steady state concentration in its formation from dicarbonyl

$$Pt(CO)_2 + CO \rightleftharpoons Pt(CO)_3$$

and its disappearance

$$Pt(CO)_3 + CO \rightleftharpoons Pt(CO)_4$$

to the tetracarbonyl.

These tentative assignments can be confirmed by mixed carbon monoxide isotope experiments. For example, Pt atoms were cocondensed with $^{12}C^{16}O$:$^{13}C^{16}O$:Ar $\simeq$ 1:1:500 mixtures and *six* CO stretching modes were observed on deposition at 10°K (Figure 4 and Table II). The strong line at 2052 cm^{-1} yields a *single* strong $^{13}C^{16}O$ isotope line at 2007 cm^{-1} and is clearly assigned to platinum monocarbonyl, PtCO. The calculated and observed shifts for PtCO are in excellent agreement and yield a Cotton–Kraihanzel force constant k_{CO} = 17.02 mdyn/Å. That the T_2 mode of $Pt(^{12}C^{16}O)_4$ (2053 cm^{-1}) is virtually coincident with the Σ^- mode of $Pt^{12}C^{16}O$ (2052 cm^{-1}) is confirmed by the *absence* of $Pt(^{12}C^{16}O)_n(^{13}C^{16}O)_{4-n}$ (n = 1–3) mixed isotope lines on deposition of Pt atoms with the dilute $^{12}C^{16}O/^{13}C^{16}O$/Ar mixture (Figure 4).

Table II. Observed and Calculated CO Stretching Modes of $Pt(^{12}C^{16}O)_n(^{13}C^{16}O)_{2-n}$ (n = 0–2), $Pt(^{12}C^{16}O)$, and $Pt(^{13}C^{16}O)$ and Best Fit C–K[a] Force Constants

Obsd	Calcd	Assignment[b]
2063.5	2062.8	Σ^+ $Pt(^{12}C^{16}O)(^{13}C^{16}O)$
2057.2	2057.5	Σ_u^+ $Pt(^{12}C^{16}O)_2$
2015.2	2016.0	Σ^+ $Pt(^{12}C^{16}O)(^{13}C^{16}O)$
2012.2	2011.8	Σ_u^+ $Pt(^{13}C^{16}O)_2$
2052.0		Σ^+ $Pt(^{12}C^{16}O)$
2007.0		Σ^+ $Pt(^{13}C^{16}O)$

[a] Cotton–Kraihanzel. [b] Best fit C–K CO force constants for $Pt(CO)_2$ were k_{CO} = 17.18 and $K_{CO,CO}$ = 0.08 mdyn/Å. The best fit C–K CO force constant for PtCO is k_{CO} = 17.02 mdyn/Å.

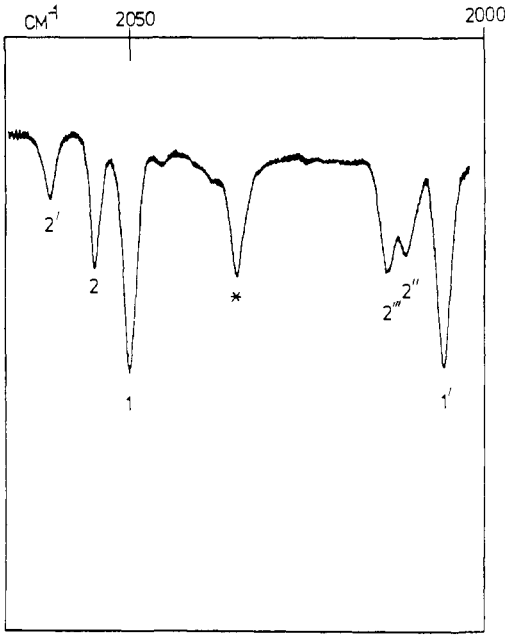

Figure 4. The matrix infrared spectrum of the products of the cocondensation reaction of Pt atoms with $^{12}C^{16}O$:$^{13}C^{16}O$:Ar = 1:1:500 at 10°K. The asterisk indicates $Pt(CO)_n(CO_2)_m$ impurity (see text).

The weaker line originally at 2057.2 cm^{-1} in $^{12}C^{16}O$/Ar mixtures yields a characteristic *doublet* of *doublets* isotope pattern with lines at 2063.5, 2057.2 and 2015.2, 2012.2 cm^{-1} (Table II and Figure 4) and identifies platinum dicarbonyl. Using these four CO stretching modes, a least-squares analysis of the data was applied to the frequencies assuming the Cotton–Kraihanzel force field approximation and a linear ($D_{\infty h}$) $Pt(CO)_2$ molecule. The best fit force constants were computed to be k_{CO} = 17.18 and $k_{CO,CO}$ = 0.08 mdyn/Å. The calculated frequencies (Table II) were in excellent agreement with those observed and provide convincing evidence for the correctness of our vibrational assignments and the authenticity of $Pt(CO)_2$.

Owing to the low absorbance of the line at 2049.0 cm^{-1}, it was not possible to obtain definitive mixed isotope data to confirm the assignment of this line to the tricarbonyl species. However, warm-up experiments (20–25°K) performed on the $^{12}C^{16}O$:$^{13}C^{16}O$:Ar $\simeq$1:1:500 matrix yielded at least *one* line at 2022.4 cm^{-1} that could not be associated with any of the isotopic lines of the mono-, di-, or tetracarbonyl species (see Table III) at this particular stage of the warm-up. Aside from the lines at 2049.0 and 2022.4 cm^{-1}, none of the lines belonging to the mixed isotopic complexes of the form $Pt(CO)_3$ were observed (six lines are expected altogether). Presumably this was due to the fact that these "missing" lines overlapped with others belonging to PtCO, $Pt(CO)_2$ and $Pt(CO)_4$, all of which were present at this stage of the warm-up (see Table III). In order to test this hypothesis, we used a value of k_{CO} for $Pt(CO)_3$ (17.24 mdyn/Å) obtained by interpolation in Figure 5. This was possible because k_{CO} values for the species PtCO, $Pt(CO)_2$, and $Pt(CO)_4$ had been previously obtained. $k_{CO,CO}$ was then calculated (0.28

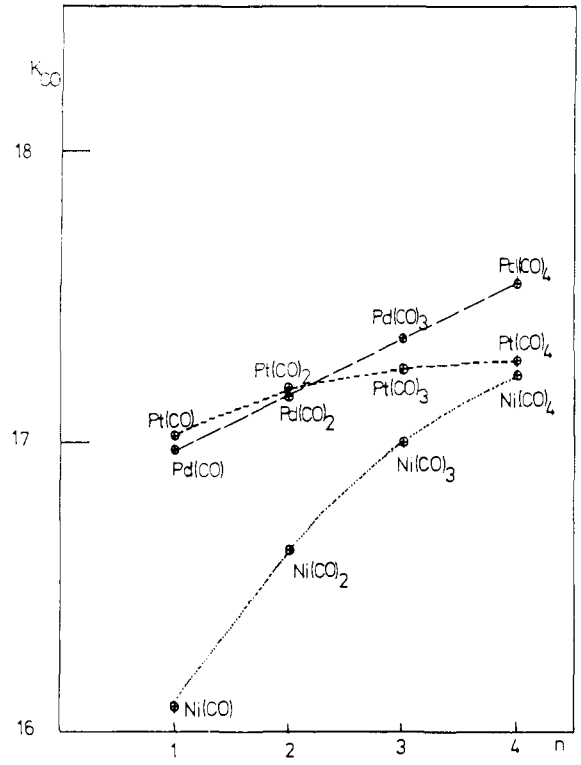

Figure 5. Graphical representation of the Cotton-Kraihanzel CO bond stretching force constant k_{CO}^{M} for $M(CO)_n$ (where M = Ni, Pd, or Pt; n = 1-4) as a function of the coordination number n.

Table III. Calculated and Observed CO Stretching Modes of $Pd(^{12}C^{16}O)_n(^{13}C^{16}O)_{3-n}$ (n = 0-3)

Obsd	Calcd[a]	Assignment
d	2090.0	(A_1) $Pt(^{12}C^{16}O)_2(^{13}C^{16}O)$
d	2078.5	(A_1) $Pt(^{12}C^{16}O)(^{13}C^{16}O)_2$
2049.0	2049.0	(E′) $Pt(^{12}C^{16}O)_3$, (B_2) $Pt(^{12}C^{16}O)_2(^{13}C^{16}O)$
2022.4[b]	2023.2	(A_1) $Pt(^{12}C^{16}O)(^{13}C^{16}O)_2$
c	2012.0	(A_1) $Pt(^{12}C^{16}O)_2(^{13}C^{16}O)$
a	2003.5	(E′) $Pt(^{13}C^{16}O)_3$, (B_2) $Pt(^{12}C^{16}O)(^{13}C^{16}O)_2$

[a] Expected to be hidden by the strong band of $Pt(^{13}C^{16}O)$ at this stage of the warm-up experiment and later by $Pt(^{13}C^{16}O)_4$. [b] Appears with *too large* an intensity at this stage of the warm-up experiment to be assigned to a $^{13}C^{16}O$ isotope line of $Pt(^{12}C^{16}O)_2(^{13}C^{16}O)_2$ at 2021.9 cm^{-1} (see Table I.). [c] Expected to be hidden by the $^{13}C^{16}O$ isotope lines of $Pt(^{13}C^{16}O)_2$ and $Pt(^{12}C^{16}O)(^{13}C^{16}O)$ at 2012.2 and 2015.2 cm^{-1}, respectively (see Table II), at this stage of the warm-up experiment. [d] Expected to appear with low intensities and were not observed. [e] Calculated for k_{CO} = 17.24 and $k_{CO,CO}$ = 0.28 mdyn/Å.

mdyn/Å) by assigning the line at 2049.0 cm^{-1} to the E-CO stretching mode of $Pt(^{12}CO)_3$ assuming D_{3h} symmetry. The expected positions of the isotope lines for $Pt(CO)_3$ resulting from that calculation are listed in Table III. It is gratifying to note that all lines but for those at 2049.0 and 2022.4 cm^{-1} are predicted to be hidden by lines belonging to other species in the matrix. Despite this fact we cannot regard $Pt(CO)_3$ to be unambiguously characterized.

Metal–Ligand Stretching Modes. When the T_2 CO stretching mode of $Pt(CO)_4$ was arranged to be fully absorbing, it was possible to observe a weak absorption at 304 cm^{-1}. Similar experiments with $Ni(CO)_4$ and $Pd(CO)_4$ yielded lines at 435 and 258 cm^{-1}, respectively.[4] Unfortunately, it was not possible to observe M–C stretching modes for the lower carbonyls.

Molecular $M(^{12}C^{16}O)_4$ has four infrared active vibrations of T_2 symmetry: ν_{CO}, stretching; δ_{M-C-O}, bending; ν_{M-C}, stretching; δ_{C-M-C}, bending. By analogy with $Ni(^{12}C^{16}O)_4$ which shows the δ_{C-Ni-C} at 80 cm^{-1},[14] it is unlikely that this mode would be observed for the Pd and Pt analogs as the range of the spectrometer was 4000–200 cm^{-1}. The CO stretching modes have been assigned for all three metals. Therefore, it remains to assign the low frequency modes observed for $Pt(^{12}C^{16}O)_4$ (304 cm^{-1}), and for the purposes of comparison $Pd(^{12}C^{16}O)_4$ (258 cm^{-1}), to either the ν_{M-C} stretching or δ_{M-C-O} deformational mode. In $Ni(^{12}C^{16}O)_4$ the corresponding ν_{Ni-C} and δ_{Ni-C-O} vibrations lie at 423.1 and 458.9 cm^{-1}.[14] It is noteworthy that the ν_{Ni-C} stretching mode is by far the most intense. It thus seems reasonable to deduce that the bands observed at 258 and 304 cm^{-1} for $Pd(^{12}C^{16}O)_4$ and $Pt(^{12}C^{16}O)_4$ are the T_2 Pd–C and Pt–C stretching modes, respectively.

Clearly there are insufficient data for $Pd(CO)_4$ and $Pt(CO)_4$ to permit a complete vibrational analysis. However, it is interesting to note that a full analysis[14] of $Ni(CO)_4$ yields a potential energy function which indicated that there was very little coupling between the ν_{Ni-C} stretching and δ_{Ni-C-O} deformational modes. Therefore, a reasonable estimate of the Pd–C and Pt–C bond stretching force constants may be obtained using a simple analysis in which $M(^{12}C^{16}O)_4$ is considered to be MX_4 where X is a mass equal to the mass of CO and using the equation

$$\lambda_{T_2} = k_{M-C}(\mu_X + (4/3)\mu_M)$$

where μ_X and μ_M are the reciprocal masses of X ($^{12}C^{16}O$ = 28) and M, respectively, and k_{MC} is the M–C bond stretching force constant. The values obtained for the Ni–C, Pd–C, and Pt–C force constants using this approximation are respectively 1.80, 0.82, and 1.28 mdyn/Å (see Table IV). It is reassuring to note that the full analysis[14] for $Ni(^{12}C^{16}O)_4$ based on all vibrations yields a Ni–C bond stretching force constant of 1.98 mdyn/Å as compared with 1.80 mdyn/Å obtained from the approximation. The close agreement between these two values suggests that within the limits of the simple analysis, the low values of the Pd–C and Pt–C bond stretching force constants are significant and consistent with the low thermal stability of $Pd(CO)_4$ and $Pt(CO)_4$ compared with $Ni(CO)_4$ (see the later section for a detailed discussion of bonding and stabilities).

Table IV. Ligand and Metal Ligand Force Constant and Frequency Data for $M(CO)_4$ (Where M = Ni, Pd, or Pt)

	ν_{CO}, cm^{-1}	ν_{M-C}, cm^{-1}	k_{CO},[a] mdyn/Å	k_{MC},[b] mdyn/Å	Ref
Ni	2052	435	17.23	1.80	6
Pd	2070	258	17.55	0.82	3
Pt	2053	304	17.28	1.28	*c*

[a] Cotton–Kraihanzel force constant. [b] Determined using the approximation which treats $M(CO)_4$ as an MX_4 molecule with X = mass 28. [c] This study.

(14) L. H. Jones, R. S. McDowell, and M. Goldblatt, *J. Chem. Phys.*, **48**, 2663 (1968).

Table V. Comparison of Frequency and Bond Stretching Force Constant Depressions for Binary Carbonyl Complexes of Nickel, Palladium, and Platinum[a]

$M(CO)_n$	n[b]	$\Delta\nu_{CO}$	ΔF_{CO}	$\Delta H_c = n(\Delta F_{CO})$
Ni	1	142	2.37	2.37
	2	171	1.83	3.66
	3	121	1.46	4.38
	4	86	1.23	4.92
Pd	1	88	1.49	1.49
	2	94	1.30	2.60
	3	78	1.11	3.33
	4	68	0.92	3.68
Pt	1	86	1.44	1.44
	2	80	1.28	2.56
	3	90	1.22	3.66
	4	85	1.18	4.72

[a] See text for notation. [b] Coordination number.

Concentration Behavior, Warm-Up Characteristics, and Stabilities of the Binary Carbonyl Complexes of Nickel, Palladium, and Platinum. It was observed that the *major* product of the cocondensation reaction of Ni, Pd, and Pt atoms with dilute CO/Ar mixtures ($\leq$1:250) at 4.2–10°K was always the monocarbonyl MCO. Warm-up studies of these matrices showed significant intensity changes during diffusion which were the result of the successive addition of carbon monoxide to lower carbonyl species to yield ultimately the tetracarbonyl $M(CO)_4$. Deposition of metal atoms into pure CO or concentrated CO/Ar mixtures yielded the tetracarbonyl as the major product.

From our experiences with binary dinitrogen and carbonyl complexes it has become apparent that the relative thermodynamic stabilities of a series of similar compounds can be qualitatively related to the difference between the force constant of the free ligand and the respective Cotton–Kraihanzel (C–K) force constant. A bond energy function H_c was previously defined[15] by

$$\Delta H_c = n\Delta F_{CO}$$

where $\Delta F_{CO} = k^L - k_{C-K}$, k^L and k_{C-K} being the free ligand and C–K bond stretching force constants, respectively, and n the coordination number with respect to the ligand. It was previously speculated that ΔH_c gives a measure of the enthalpy of decomposition of the appropriate compound for which it was measured. The computed values of ΔH_c for the binary carbonyl complexes of Ni, Pd, and Pt as a function of n are shown in Figure 6 and Table V. The results for $Ni(CO)_n$, $Pd(CO)_n$, and $Pt(CO)_n$ are seen to *parallel* their warm-up behavior and confirm that the most stable complexes are those with the highest stoichiometry, namely $Ni(CO)_4$, $Pd(CO)_4$, and $Pt(CO)_4$. It is also interesting to note that the order of relative thermodynamic stabilities for corresponding Ni, Pd, and Pt complexes parallels exactly the order of stability of the respective tetracarbonyls, as measured by their metal–carbon bond stretching force constants, that is, $Ni(CO)_m > Pt(CO)_m \geq Pd(CO)_m$ and $k_{NiC} > k_{PtC} > k_{PdC}$ which, as expected, parallels in an inverse fashion the C–K CO bond stretching force constants, namely

$$k_{CO}^{Ni(CO)_m} < k_{CO}^{Pt(CO)_m} \lesssim k_{CO}^{Pd(CO)_m}$$

(15) E. P. Kündig, M. Moskovits, and G. A. Ozin, *Can. J. Chem.*, in press.

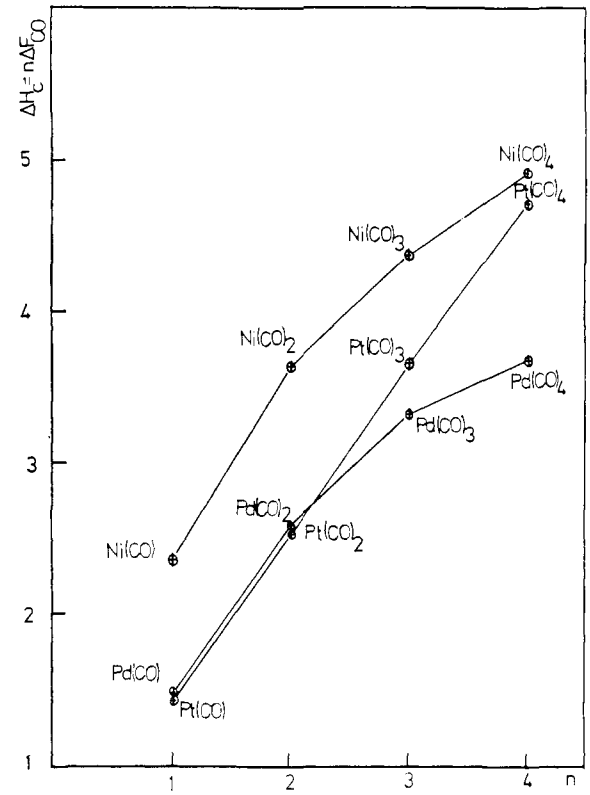

Figure 6. Graphical representation of $\Delta H_c = n(\Delta F_{CO})_M$ for $M(CO)_n$ (where M = Ni, Pd, or Pt; n = 1–4) as a function of the coordination number n.

Force Constants and Bonding in $M(CO)_n$ (Where M = Ni, Pd, and Pt, n = 1–4). The Cotton–Kraihanzel CO bond stretching force constants for $M(CO)_n$ (where M = Ni, Pd, or Pt; n = 1–4) as a function of coordination number n are illustrated graphically in Figure 5. For all three metals, a monotonic increase in k_{CO} on passing from the monocarbonyl MCO to the tetracarbonyl $M(CO)_4$ is observed. From previous work it is known that carbon monoxide bonds to a transition metal by two mechanisms: (i) a σ bond is created by electron donation from the carbonyl 5σ orbital to the unfilled metal orbitals, (ii) a π bond is created by electron donation from the filled metal d orbitals to the unfilled 2π carbonyl orbitals. Examination of the overlap populations of the 5σ and 2π orbitals has shown that both are antibonding in character. Consequently, electron donation from the 5σ orbital will strengthen the carbon–oxygen bond, while electron donation to the 2π will weaken the bond. Therefore, the resultant C–O bond strength depends on the competition between these two bonding processes.

Fenske[16] has shown that in a series of related metal carbonyl complexes the CO stretching C–K force constant depends in a linear fashion on both the 5σ and 2π orbital populations. Recently too we have shown that writing the C–K CO stretching force constant in the form

$$f_{CO} = d + |a|(\sigma - \gamma\pi)$$

where d and γ are positive constants and σ and π are the decrease in 5σ population and the 2π population of CO, respectively, allowed us to explain satisfactorily the

(16) M. B. Hall and R. F. Fenske, *Inorg. Chem.*, **11**, 1619 (1972).

bonding character of the series of compounds $Ni(CO)_m(N_2)_{4-m}$.[15] Accordingly we assume that the expression

$$K_n^M = d + |a|(\sigma_n^M - \gamma\pi_n^M) \quad (1)$$

where K_n^M refers to the CO stretching force of the species $M(CO)_n$, M being Ni, Pd, and Pt, holds for the present set of complexes. K_n^M increases if either σ_n^M increases or π_n^M decreases. Thus eq 1 indicates that the monotonic increase in K_n^M with increasing n for M = Ni, Pd, and Pt must be due to the decreasing π backbonding as one proceeds from MCO to $M(CO)_4$, since it is not considered likely that σ donation would increase with increasing coordination number.

Equation 1 also allows us to determine the relative π acid characteristics of CO toward Ni, Pd, or Pt. Turning our attention specifically to the tetracarbonyl species we find that

$$K_4^{Pd} > K_4^{Pt} > K_4^{Ni}$$

Thus

$$(\sigma_4^{Pd} - \gamma\pi_4^{Pd}) > (\sigma_4^{Pt} - \gamma\pi_4^{Pt}) > (\sigma_4^{Ni} - \gamma\pi_4^{Ni}) \quad (2)$$

Now the energies of the 3d of Ni, 4d of Pd, and 5d of Pt are reported to be in the order

$$4d(Pd) > 5d(Pt) > 3d(Ni)$$

One would then intuitively expect the relative σ-donor abilities of CO toward the three metals to be in the order

$$\sigma_4^{Pd} < \sigma_4^{Pt} < \sigma_4^{Ni} \quad (3)$$

This speculation is further strengthened by the observation that the Allred–Rochow electronegativities are reported to be $\chi(Pd) < \chi(Pt) < \chi(Ni)$. Combining inequality 2 with inequality 3 yields the result

$$\pi_4^{Pd} < \pi_4^{Pt} < \pi_4^{Ni}$$

We conclude therefore that both σ-donor and π-acceptor abilities of CO to M in $M(CO)_4$ go in the order

$$Ni > Pt > Pd$$

where the "is greater than" sign is to be read "is better than." This result is, once again, consistent with the thermal stabilities of the three tetracarbonyl species.

A similar analysis for the mono-, di-, and tricarbonyl species produces the same result.

The Charge on the Metal Atom. It is at once obvious that the quantity $\sigma_n^M - \pi_n^M$ is the charge, including sign, on the CO ligand in the species $M(CO)_n$. In particular the charge on a CO ligand, Q_{CO}^M, in the tetracarbonyl species $M(CO)_4$ is given by

$$Q_{CO}^M = \sigma_4^M - \pi_4^M \quad (4)$$

Moreover, eq 1 may be rewritten for the particular case of the tetracarbonyls as

$$(K_4^M - d)/|a| = \sigma_4^M - \gamma\pi_4^M \quad (5)$$

Equations 4 and 5 form two simultaneous equations in two unknowns which could be solved for σ_4^M and π_4^M if the quantities Q_{CO}^M, d, γ, and $|a|$ were known. The last set of quantities may be evaluated from Fenske's data assuming that they may be carried over to binary tetracarbonyls from the octahedral mixed carbonyl halides for which they were calculated.[16] Thus d, γ, and $|a|$ equal respectively 16.805, 1.234, and 9.504. The quantity Q_{CO}^M is in general not available except for the case of $Ni(CO)_4$ for which SCF–MO calculations have been performed. Hillier[17] reports a value of 0.24 electron for the charge on each CO in $Ni(CO)_4$ (not equally distributed) while Nieuwpoort[18] reports 0.23 electron. Using this value in eq 4 and combining with eq 5 one obtains $\sigma_4^{Ni} = 1.07$ and $\pi_4^{Ni} = 0.83$ which are, respectively, the number of σ-donated and π-accepted electrons by each CO in $Ni(CO)_4$.

Because MO calculations have not been performed on $Pd(CO)_4$ and $Pt(CO)_4$, one cannot solve for σ_4^M and π_4^M for these complexes in the same manner as was done for $Ni(CO)_4$. We therefore make the assumption that σ_4^M is proportional to χ_M, the Allred–Rochow electronegativities of the corresponding metal, and solve for π_4^M from eq 5. The results are given in Table VI. These calculations indicate that Pd and Pt do not differ markedly in their donor and acceptor properties. Ni, on the other hand, is a substantially better donor and acceptor than the former two metals resulting in the observed thermal stability of $Ni(CO)_4$. It is intriguing that the charge on the ligand (hence the charge on the metal which is approximately equal to $-4Q_{CO}^M$) does not vary appreciably on going from $Ni(CO)_4$ to $Pd(CO)_4$ to $Pt(CO)_4$. A similar result was reported by Hillier[17] for $Ni(CO)_4$, $Cr(CO)_6$, and $Fe(CO)_5$.

Table VI. Calculated σ_4^M and π_4^M Values and Total Charge Q_{CO}^M on CO for $Ni(CO)_4$, $Pd(CO)_4$, and $Pt(CO)_4$

M	χ_M[a]	σ_4^M	π_4^M	Q_{CO}^M[b]
Ni	1.75	1.07	0.83	0.24
Pd	1.35	0.83	0.61	0.22
Pt	1.44	0.88	0.67	0.21

[a] Allred–Rochow electronegativities. [b] Obtained from eq 4.

The observed values for K_4^M as well as those of σ_4^M and π_4^M indicate a reversal in order when going from $Pd(CO)_4$ to $Pt(CO)_4$. This may be a manifestation of the lanthanide contraction resulting from the poor screening by the filled 4f levels in Pt resulting in an increased electron–nuclear attraction energy and a drop in the energy levels on passing from Pd to Pt.

Relationship between MCO and CO Chemisorbed on M (Where M = Ni, Pd and Pt) and Comparison with the Corresponding Data of MN_2 and N_2 Chemisorbed on M. We have recently suggested[15,19] that a connection exists between our earlier studies of NiN_2, PdN_2, PtN_2, and N_2 chemisorbed on Ni, Pd, and Pt, respectively. It was noted, for example, that the frequency of the N_2 stretching modes was in the order Ni < Pt < Pd for both MN_2 and N_2 chemisorbed on M. It was also observed that in all three cases ν_{NN} was *higher* for chemisorbed N_2 than for the corresponding MN_2 molecule.

In attempting to draw similar conclusions regarding our MCO (M = Ni, Pd, Pt) and corresponding CO chemisorbed on bulk Ni, Pd, and Pt, a difficulty is encountered. The spectra of CO chemisorbed on M consists not of one but of at least two absorptions, one lying in the terminal CO stretching region while the other lies in the bridge-bonded CO stretching region.

(17) I. H. Hillier, *J. Chem. Phys.*, **52**, 1948 (1970).
(18) W. C. Nieuwpoort, *Phillips Res. Rep., Suppl.*, **6**, 1 (1965).
(19) M. Moskovits and G. A. Ozin, *J. Chem. Phys.*, **58**, 1251 (1973).

Table VII. Comparison between CO Stretching Frequencies of Carbon Monoxide Chemisorbed on Ni, Pd, and Pt and the Analogous MCO Complexes

M	ν_{CO} chemisorbed CO[a]	ν_{CO} chemisorbed MCO[b]	$\Delta\nu_{ChCO}$	$\Delta\nu_{MCO}$	$(\Delta\nu_{MCO}/\Delta\nu_{ChCO})_M$	$(\Delta\nu_{MN_2}/\Delta\nu_{ChN_2})_M$[c]
Ni	2032.5	1996	105.5	142	1.35	1.90
Pd	2053.4	2050	84.6	88	1.04	1.70
Pt	2070.4	2052	67.6	86	1.27	1.60

[a] Reference 20. [b] This study. [c] The corresponding dinitrogen data have been included for the purposes of comparison.

Moreover, reported values for the CO stretching absorption associated with chemisorbed CO on these metals vary from author to author. In order to obtain at least a self-consistent comparison we chose the only available study in which chemisorption on all three metals was investigated using the same techniques.[20] In each case we chose the absorption at the highest frequency to be that due to terminal chemisorbed CO.

The results are compiled in Table VII, which indicates once again that ν_{CO} is higher for CO chemisorbed on M than ν_{CO} for the corresponding MCO species. Included in the table are also values of the ratio $R_{CO}^{M} = (\Delta\nu_{MCO}/\Delta\nu_{ChCO})_M$ where $\Delta\nu_{MCO}$ and $\Delta\nu_{ChCO}$ are the frequency decreases in going from free CO to respectively MCO and chemisorbed CO. For comparison the ratios $R_{N_2}^{M} = (\Delta\nu_{MN_2}/\Delta\nu_{ChN_2})_M$ referring to the corresponding dinitrogen complexes are also included. In every case the ratio for the CO system is substantially *smaller* than for the N_2 system. The reason for this is as follows.

Define the quantities K_{CO}, K_{1CO}^{M}, and K_{ChCO}^{M} to be the force constant for free CO, the C–K force constant for MCO, and the C–K force constant for chemisorbed CO on M. We have therefore

$$\frac{K_{CO} - K_{1CO}^{M}}{K_{CO} - K_{ChCO}^{M}} = \frac{(\nu_{CO}^{2} - \nu_{MCO}^{2})}{(\nu_{CO}^{2} - \nu_{ChCO}^{2})} = \frac{(\nu_{CO} - \nu_{MCO})(\nu_{CO} + \nu_{MCO})}{(\nu_{CO} - \nu_{ChCO})(\nu_{CO} + \nu_{ChCO})}$$

Because the factor on the extreme right of the above equation is approximately equal to unity

$$R_{CO}^{M} \simeq (K_{CO} - K_{1CO}^{M})/(K_{CO} - K_{ChCO}^{M}) \quad (6)$$

Substituting eq 1 into eq 6 we obtain

$$R_{CO}^{M} \simeq 1 + |a|\left[\frac{\gamma\Delta\pi_{CO} - \Delta\sigma_{CO}}{K_{CO} - K_{ChCO}^{M}}\right] \quad (7)$$

where $\Delta\pi_{CO} = \pi_{1CO}^{M} - \pi_{ChCO}^{M}$, that is, the decrease in π-accepted charge in going from MCO to chemisorbed CO, and $\Delta\sigma_{CO} = \sigma_{1CO}^{M} - \sigma_{ChCO}^{M}$, that is, the decrease in σ-donated charge sustained during the same process.

In ref 15 we indicated that an equation of the form

$$f_{N_2} = d' - a'(\sigma + \gamma'\pi)$$

described the N–N stretching force constant in binary dinitrogen complexes. Defining the quantities K_{N_2}, $K_{1N_2}^{M}$, and $K_{ChN_2}^{M}$ to be the force constant of free N_2 and the C–K N–N stretching force constants of MN_2 and N_2 chemisorbed on M, respectively, we can show by a similar argument that

$$R_{N_2}^{M} \simeq (K_{N_2} - K_{1N_2}^{M})/(K_{N_2} - K_{ChN_2}^{M}) \quad (8)$$

and that

$$R_{N_2}^{M} \simeq 1 + a'\left[\frac{\gamma'\Delta\pi_{N_2} + \Delta\sigma_{N_2}}{K_{N_2} - K_{ChN_2}^{M}}\right] \quad (9)$$

where $\Delta\pi_{N_2}$ and $\Delta\sigma_{N_2}$ are defined by analogy with $\Delta\pi_{CO}$ and $\Delta\sigma_{CO}$.

It is at once clear that $R_{N_2}^{M} > R_{CO}^{M}$ because the second term in eq 7 is of the form $\Delta\pi - \Delta\sigma$ while that of eq 9 is of the form $\Delta\pi + \Delta\sigma$. (Note that since $(K_{CO} - K_{ChCO}^{M}) < (K_{N_2} - K_{ChN_2}^{M})$ the relative magnitude of $R_{N_2}^{M}$ to R_{CO}^{M} cannot be explained by the magnitude of the denominators in eq 7 and 9.)

The implication of the above result is that there are *both* σ and π decreases accompanying passage from either the monocarbonyl or monodinitrogen complex to the chemisorbed ligand on M. Moreover, $\gamma\Delta\pi_{CO}$ must be greater than $\Delta\sigma_{CO}$ in order to explain R_{CO}^{M}'s being greater than unity. Since γ is approximately unity we conclude that π backbonding is decreased *more* than is σ bonding when going from MCO to chemisorbed CO.

Assuming one can extend our previously stated argument relating $n\Delta F_{CO}$ with ΔH_c to the case of chemisorbed CO, the data indicate that the metal–carbon bond strength is lower in chemisorbed CO than in the corresponding MCO complex and takes the order Ni > Pt > Pd. One concludes from these data that a great deal of insight into the bonding of CO and N_2 to surface metal atoms may be obtained by comparison with the corresponding MCO and MN_2 molecules and once again would support the view that the forces which bind molecules to metal surfaces upon chemisorption are in many ways similar to those operating in conventional metal–ligand coordination complexes.

Acknowledgments. We wish to thank the Research Corporation and the National Research Council of Canada for financial support.

(20) R. P. Eischens, W. A. Pliskin, and S. A. Francis, *J. Chem. Phys.*, 22, 1786 (1954).